Influence of surface charges on the rupture of black lipid membranes

Anke Diederich, Günther Bähr, and Mathias Winterhalter*
Department of Biophysical Chemistry, Biozentrum of the University of Basel, Klingelbergstrasse 70, CH-4056 Basel, Switzerland
(Received 26 June 1998)

We investigate the influence of surface charges on the rupture of black lipid membranes (BLM). Rupture is induced by short electric voltage pulses across the membrane. The average voltage necessary to induce breakdown gives information on the energy barrier of defect formation. The rapid transmembrane voltage decay during rupture allows one to evaluate the kinetics of defect widening. The breakdown voltage is about the same for BLM made of lipids with phosphatidylserine headgroups and for BLM made of lipids with phosphatidylcholine headgroups. Moreover, the breakdown voltage is independent of the ionic strength of the aqueous medium surrounding the BLM. This indicates that the stability of the BLM is not dominated by mutual electrostatic repulsion of the headgroups. However, the breakdown voltage depends on the type of the hydrophobic chains of the lipids. Palmitoyl-oleoyl (PO) membranes require ~100-mV smaller breakdown voltages compared to diphytanoyl (DPh) membranes. Surprisingly, the rupture kinetics depends on the hydrocarbon chains. It was found to be four times faster for DPh than for PO membranes, and independent of the type of headgroup. [S1063-651X(98)15210-8]

PACS number(s): 87.45.−k, 82.65.Dp, 62.20.Mk, 83.50.Lh

INTRODUCTION

Electroporation techniques are based on the fact that the structural integrity of lipid membranes is affected by electric fields. Detailed investigations concerning this phenomenon were done almost 20 years ago on free-standing planar lipid membranes [1,2]. It was shown that the application of a certain voltage causes a sudden and irreversible breakdown of the membrane. The average voltage necessary to disrupt a membrane is commonly called the breakdown voltage, and depends on the lipid composition of the membrane. Several models describe the influence of *trans*-membrane electric fields on the structure and stability of membranes [3–8]. The initial process of membrane rupture is nevertheless still a matter of debate. The application of a voltage across a membrane causes so-called Maxwell stresses on the membrane. They act as real forces at the membrane-water boundaries, and are balanced by mechanical stresses. Experimental observations indicate, however, that the electric-field-induced Maxwell tension is too small to cause membrane rupture [9]. More recent models are therefore based on the assumption that a *trans*-membrane electric field reduces the edge energy necessary to create a defect [10,11].

The equivalency of electric-field-induced stresses with mechanical applied ones was shown on giant vesicles of selected lipid composition [9]. It was demonstrated that both externally applied tensile and electrocompressive stresses sum up in electroporation experiments. Therefore, electroporation experiments contain information on the mechanical properties of membranes. Black lipid membranes (BLM) are a particularly well suited model membrane system for rupture experiments as defect formation can be easily monitored from the increase of the membrane conductivity during rupture [1,3,12].

Currently we investigate the influence of monovalent and multivalent ions on the rupture process of surface-charged BLM. Due to the long-range mutual electrostatic repulsion between the net-charged lipid headgroups, one expects these membranes to have smaller stability and breakdown voltages compared to neutral membranes. The question of whether these electrostatic repulsive forces significantly alter the stability of membranes is rather fundamental, as most natural occurring membranes have net-charged lipids incorporated into the bilayer. These lipids are often accumulated in one leaflet of the membrane, and cause a intrinsic *trans*-membrane potential which adds to an externally applied field [13]. The membrane stability depends in this case on the intrinsic electric field as well as on the mechanical stress caused by the repulsion of the net-charged headgroups. The repulsion is due to the electric field which acts between the dissociated headgroups and their counter ions in the aqueous phase. Within Gouy-Chapman theory, this additional stress σ is described by [14]

$$\sigma=\left(\frac{2kT}{e}\right)^2 \frac{\varepsilon_w\varepsilon_0}{\lambda_{\mathrm{Debye}}}[q-1] \quad \text{where} \quad q=\sqrt{1+p^2},$$

$$p=\frac{\sigma^* e}{2\varepsilon\varepsilon_0 kT}\lambda_{\mathrm{Debye}},$$

$$\lambda_{\mathrm{Debye}}=\left(\frac{\varepsilon_w\varepsilon_0 kT}{2n_0e^2}\right)^{1/2}.$$

Here kT is the Boltzmann factor, σ^* the surface charge density, e the elementary charge and n_0 the ion concentration. The surface potential is related to the surface charge density by

*FAX: 41-61-267 2189. Electronic address: Winterhalter@ubaclu.unibas.ch

$$\phi = \left(\frac{2kT}{e}\right) \ln[q + p]. \quad (1)$$

Equation (1) predicts, e.g., for a pure phosphatidylserine (PS) membrane with a surface charge density $\sigma^* = 0.25$ A s/m^2 at a Debye length of $\lambda_{\text{Debye}} = 1$ nm, a surface potential of about 130 mV and a repulsive tension of about 11 mN/m. On the other hand, Needham and Nunn showed experimentally that most membranes disrupt after applying a mechanical stress of only 2–6 mN/m [15]. On the basis of Gouy-Chapman theory, it should therefore be impossible to form stable PS vesicles or BLM in water containing $\leqslant$100 mM monovalent ions. However, it is a fact that PS vesicles as well as BLM can be formed readily at these KCl concentrations. On the other hand, it is known from the literature that surface charges can affect the structure or mechanical properties of membranes. Calorimetric studies on the influence of *p*H on the phase transition temperature of selected lipid dispersions indicate for example that high surface charge densities in membranes lower their phase transition temperature [16–18].

Here, we direct our attention to the rupture kinetics of BLM. Recently, we adapted an electroporation method which allows one to follow the defect widening with a time resolution of about 1 μs [3,19]. In this method, we apply single short voltage pulses across the lipid membrane and record the voltage decay after each pulse. By increasing the voltage in small steps, we induce single defects which increase in size or reseal depending on the size of the initial defect. The time course of the voltage decay allows conclusion on the kinetics of the defect widening. Previous investigations on pure lipid bilayers showed a linear increase of conductance with time [3,19]. From this increase, radial pore widening velocities in the range of 0.1–0.3 m/s could be obtained. According to our model, the linear increase of pore radius in time indicates that the pore widening kinetics is determined by the inertia of the film [19]. Recently, we demonstrated that diverse high molecular weight polymers which decorate the surface of BLM reduce significantly the rupture velocity of the membranes. For example *F*-actin polymerized on stearylamine-containing membranes reduced the rupture velocity several orders of magnitude [20]. The radius of the pores induced in such membranes increases exponentially instead of linearly in time. This allows the determination of the two-dimensional shear viscosity of the decorated membranes. A change in the rupture behavior was also observed on negatively charged membranes by decoration with polylysine. With an increasing degree of polymerization of the polyelectrolyte, both the rupture kinetics and the breakdown voltage of the decorated BLM became significantly smaller [13].

In the present study, we compare the rupture behavior of negatively charged membranes to the rupture behavior of Zwitter-ionic membranes for different ionic strengths of the aqueous surrounding. Finally, we discuss the rupture kinetics of the different membranes with respect to the validity of our model assumptions.

MATERIALS AND METHODS

Diphytanoyl-phosphatidylcholine (DPhPC), diphytanoyl-phosphatidylserine (DPhPS), 1-palmitoyl-2-oleoyl-*sn*-glycero-3-phosphocholine (POPC), and 1-palmitoyl-2-oleoyl-*sn*-glycero-3-[phospho-L-serine] (POPS) were purchased from Avanti Polar Lipids (Alabaster, Alabama) with purity >99%, and used without further purification. The electrolyte contained ion-exchanged water (NANOpure, Barnstead) with specific resistance >17 MΩ cm and specified amounts of KCl (*pro analysi*) from Merck (Darmstadt, Germany). The membrane forming solution contained 1-wt % lipid in *n*-decane (Fluka). In the case of POPS, we added small amounts of 1-butanol p.a. from Merck for better solubilization of the lipids to the membrane forming solution. The solution used for prepainting contained 1-wt % lipid in chloroform (p.a.) obtained from Merck. In one set of control experiments we varied the water activity by dissolving 8 M urea (Merck) or 10-wt % poly(ethylene-glycol) 2000 (Fluka) in the electrolyte.

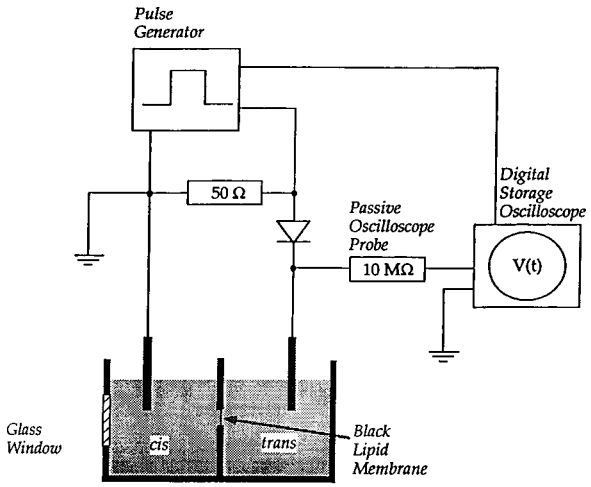

FIG. 1. Scheme of the charge-pulse instrumentation to induce and record irreversible breakdown of planar lipid membranes.

Black lipid membranes

BLM of ~1-mm diameter were formed according to Mueller *et al.* [21]. Briefly, a Teflon cuvette containing two chambers was prepainted around the hole connecting both chambers with about 1 μl of the prepainting solution. After allowing 20 min for drying, each chamber was filled with 5 ml electrolyte. 1 μl of the membrane forming solution was spread on a Teflon loop and painted across the hole, leading to a separation of both chambers by a lipid membrane. The thinning of the membrane could be observed trough a glass window in the front side of the cuvette by a microscope (60-fold magnification).

Electroporation setup

Membrane rupture was initiated with the charge-pulse method described in Ref. [19]. The experimental setup is shown in Fig. 1. The Ag/AgCl electrode in the *trans* compartment is connected to a fast pulse generator (Tektronix PG 507) through a diode (reverse resistance$\gg 10^{11}$ Ω). The voltage between the *cis* and *trans* electrodes is recorded on a digital storage oscilloscope (LeCroy 9354A).

Prior to rupture, the membrane capacitance is determined by charging the BLM with a rectangular pulse of 10-μs du-

ration to a voltage of about 100 mV. The value of the membrane capacitance is calculated from the *RC* time constant of the exponential discharge process of the membrane across the 10-MΩ resistance of the passive oscilloscope probe. An irreversible breakdown is initiated by charging the membrane with rectangular 250–800-mV voltage pulses of 10-μs duration. In order to avoid formation of multiple pores, we start to charge the membrane with a small voltage of 250 mV. Then we raise the applied voltage in 20-mV steps, applying at least five pulses per step until the membrane disrupts. In a typical rupture experiment about 20–200 pulses are applied prior to membrane rupture.

As long as the defect is small relative to the total area of the membrane, the bilayer capacitance can be considered as constant. Under this assumption the membrane conductance $G(t)$ can be calculated via [19]

$$G(t)=\frac{I(t)}{U(t)}=\frac{1}{U(t)}\frac{dQ(t)}{dt}=\frac{1}{U(t)}\frac{-d(C\cdot U(t))}{dt}$$
$$=\frac{-C}{U(t)}\frac{dU(t)}{dt}=-C\frac{d\ \ln U(t)}{dt}, \tag{2}$$

where $I(t)$ is the discharge current over the defect, $U(t)$ the *trans*-membrane voltage, $Q(t)$ the charge excess on one side of the membrane, and C the membrane capacitance. The minus sign indicates discharging of the membrane.

THEORETICAL BACKGROUND

The mechanical breakdown of a lipid membrane can be understood as an activated process [19,22,23]. In absence of an electrical field, thermal fluctuations may cause statistically pores with radius a. The further widening or resealing of such a pore is determined by two opposite energy contributions:

$$E_{\text{pore}}=2\pi a\Gamma-\pi a^2\sigma. \tag{3}$$

The first term of Eq. (3) describes the energy which is required to cut intermolecular links and to form a circular edge. The energy necessary for this process is proportional to the length of the defect $2\pi a$. The material property for this process is called the edge energy Γ. The second term in the equation is the energy gained by the widening of the pore due to the surface tension σ. The first derivative of E_{pore} with respect to a gives the forces determining the defect formation. Balancing the forces, one easily finds that pores with radii smaller than the critical radius $a^*=\Gamma/\sigma$ will reseal, while pores with radii larger than a^* will increase in size. The critical radius a^* can be estimated to be 5 nm, if the surface tension is assumed to be $\sigma=2\times10^{-3}$ N/m, and the edge energy $\Gamma=10^{-11}$ N [24–27].

In our experiments, we apply short voltage pulses across a BLM which induce surface charges at the lipid-water interface. The Maxwell stresses due to the voltage pulses are quadratically dependent on the applied voltage. It could be shown that in the presence of electric fields, the structure of Eq. (3) can be conserved if the edge energy Γ and the surface tension σ are replaced by effective quantities containing the electric field contribution [28]. The effective edge energy writes $\Gamma_{\text{eff}}=\Gamma-\varepsilon_w\varepsilon_0U^2/2\pi$, and the effective tension $\sigma_{\text{eff}}=\sigma-\varepsilon_l\varepsilon_0U^2/2d$. Here ε_w is the dielectric constant of the aqueous phase, ε_l the dielectric constant of the lipid phase, ε_0 the permittivity of the vacuum and d the membrane thickness. For a typical breakdown voltage of about 500 mV, the external electric field decreases mainly the edge energy, and only slightly the surface tension [28].

Our interpretation of rupture kinetics data is based on the assumption that the voltage pulses trigger only the formation of one pore. We derived this conclusion from the following observations [19]. Repeated determination of the conductance increase during membrane rupture under the same conditions yields a distribution around a minimal value, and multiples of it. In a few cases we observed a sudden doubling of the conductance increase during membrane rupture. This we interpreted as the occurrence of a second pore during the rupture process. If the conductance increase is due to the widening of a large number of pores, no distinct minimal value but rather a wide distribution should be observed. Moreover, we observe a very broad distribution of the delay between the end of the applied rectangular voltage pulse and membrane rupture. This again suggests rather a single event than the formation of many pores.

In case of a single pore, this pore has a large radius relative to the membrane thickness. Under these conditions the conductance $G_{\text{pore}}(t)$ of a pore can be approximated by the inverse access resistance

$$G_{\text{pore}}(t)=\frac{1}{R_{\text{pore}}}=2\kappa a(t), \tag{4}$$

where κ is the specific conductivity of the electrolyte [29]. The above equation relates the time dependence of the pore conductance to that of the pore radius. In case of a noncircular defect or multiple pores, the model approximates the total area of the defects with an equivalent circular area of radius a. In the special case of the formation of a single circular defect in the membrane this equivalent radius is equal to the radius of the pore.

The pore widening in undecorated BLM is driven by the surface tension and is limited by the inertia of the film [19,30]. The viscosity of the lipid film can in most cases be neglected. Balancing the decrease in elastic energy by inertia and dissipation during the widening of the pore yields the following time dependence for the pore radius:

$$a(t)=\left(\frac{\Phi\sigma}{d\rho}\right)^{1/2}t=\alpha t, \tag{5}$$

where Φ is a dimensionless parameter depending on unknown material flow as well as on dissipation effects. ρ represents the lipid density, d the thickness of the film, and α the radial velocity of the pore widening. In our experimental setup, we can detect a pore only from the moment when the membrane resistance becomes smaller than 10 MΩ. As the conductance of the pore is much larger than that of the intact membrane, we can equate in a good approximation the conductance of the membrane G with the conductance of the

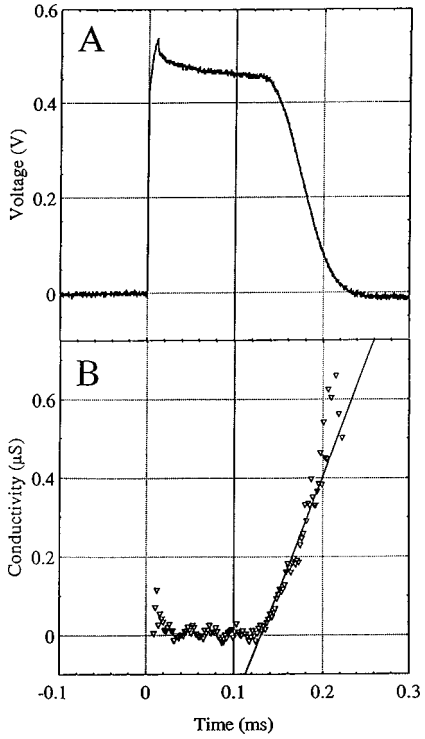

FIG. 2. (Curve *A*) time course of the membrane voltage during electric-field-induced irreversible rupture of a DPhPS membrane in 100-mM KCl. The length of the applied voltage pulse was 10 μs. The aqueous phase contained 100-mM KCl; $T=295$ K. (Curve *B*) time course of the membrane conductance calculated from the voltage curve *A*. The symbols indicate the experimental data. The solid line is a linear fit.

pore G_{pore}. A combination of Eqs. (2), (4), and (5) then yields the following expression for the radial rupture velocity:

$$\alpha = \frac{-C}{2\kappa\left(\frac{d}{dt}\ln U(t)\right)}. \tag{6}$$

EXPERIMENTAL RESULTS AND DISCUSSION

A typical time course of the *trans*-membrane voltage during rupture is shown in Fig. 2, curve *A*. The membrane was made of DPhPS in an aqueous phase containing 0.1 M KCl. An externally applied voltage pulse charged the membrane during 10 μs to a *trans*-membrane voltage of about 540 mV. This stage is followed for about 20 μs by a steep, not well understood voltage drop. This nonideal region is followed by an exponential decay of the voltage due to discharging of the membrane via the parallel 10-MΩ resistance of the passive oscilloscope probe. In this region the *RC* time constant yields information on the capacitance of the membrane. The defect formation is seen in curve *A* by a sharp kink after about 0.13 ms. This kink is followed by a superexponential voltage decay indicating the rupture of the membrane.

From this curve three different quantities can be determined. The first one is the so-called delay time, which is the time interval between the end of the externally applied voltage pulse and the onset of the superexponential decay of the voltage curve. The second quantity is the breakdown voltage causing irreversible rupture of the membrane. As the breakdown voltage we define the amplitude of the voltage shortly after the pulse when the voltage decay starts to follow the *RC* behavior. In Fig. 2, curve A, for example, a breakdown voltage of about 480 mV is read. As a third characteristic quantity, we obtain the conductance increase due to defect formation by analyzing the voltage versus time curves according to Eq. (2) (compare curves *A* and *B* of Fig. 2). As expected, the time course of the conductance of all membranes investigated in this study showed a linear increase during rupture.

TABLE I. Overview of the breakdown voltages, membrane capacitance, and rupture velocities of DPhPS membranes after chloroform prepainting of the cuvette. The aqueous medium contained 10 mM KCl; $T=295$ K.

Breakdown voltage	Membrane capacitance	Rupture velocity
630 mV	0.62 nF	25 cm/s
615 mV	0.71 nF	21 cm/s
480 mV	0.71 nF	23 cm/s
600 mV	0.72 nF	14 cm/s
710 mV	0.72 nF	17 cm/s
650 mV	0.78 nF	23 cm/s
600 mV	0.84 nF	23 cm/s
690 mV	1.04 nF	12 cm/s
400 mV	1.05 nF	17 cm/s
470 mV	1.05 nF	22 cm/s

Influence of the membrane preparation on the breakdown voltage, rupture kinetics, and capacitance of BLM

First we investigated the influence of the prepainting on the rupture process of BLM. In one set of experiments, for the prepainting we used *n*-decane as the solvent for DPhPS. In the case of *n*-decane prepainting, optical observation of the BLM revealed in most cases at their rim light-reflecting areas of silvery appearance. Prolonged waiting times or application of a series of voltage pulses did not cause the silvery edges to disappear. Light-reflecting areas were not observed in membranes where the prepainting was done with DPhPS in chloroform. The capacitance of membranes formed using chloroform prepainting was about $\sim$0.8 nF. Membranes formed using *n*-decane prepainting showed half of this capacitance for the same hole sizes. This is understandable as the capacitance is proportional to the membrane area. This finding is important for the evaluation of the influence of the membrane capacity on the rupture behavior of BLM.

We triggered rupture of these membranes as described above. Tables I and II give an overview about the experimental results obtained for chloroform and *n*-decane prepainted cuvettes. Interestingly, the breakdown voltages and the rupture velocities show no significant dependence on the membrane capacitance. This finding, together with the optical appearances of the membranes, suggests that the defects are preferentially formed in thin film regions and not in

TABLE II. Overview of the membrane capacitance, breakdown voltages, and rupture velocities of DPhPS membranes after *n*-decane prepainting. The aqueous medium contained 10 mM KCl; $T = 295$ K.

Breakdown voltage	Membrane capacitance	Rupture velocity
525 mV	0.30 nF	22 cm/s
487 mV	0.31 nF	21 cm/s
550 mV	0.33 nF	20 cm/s
494 mV	0.34 nF	27 cm/s
587 mV	0.35 nF	20 cm/s
506 mV	0.40 nF	22 cm/s
525 mV	0.54 nF	20 cm/s
581 mV	0.55 nF	24 cm/s
610 mV	0.60 nF	60 cm/s

thick regions at the edges of the membranes. Note that the breakdown voltages and rupture velocities also show no significant correlation.

Influence of the ionic strength on the breakdown voltages of PC and PS membranes

We recorded the rupture of DPhPS, DPhPC, POPS, and POPC membranes in water containing KCl in concentrations ranging from 10 mM to 3 M. The average breakdown voltages of the membranes are summarized in Table III. For DPh membranes, the average breakdown voltages were about 540 mV. Surprisingly, neither the negatively charged PS membrane nor the zwitterionic phosphatidylcholine (PC) membrane show a significant dependence on the ionic strength of the subphase. The breakdown voltages of palmitoyl-oleoyl (PO) membranes are smaller than those of DPh membranes. PO lipids show, in 2 M KCl, breakdown voltages about 50 mV smaller, and at the two lower ion concentrations values about 100 mV smaller. Again it is interesting to note that POPS and POPC membranes also have rather similar breakdown voltages at a given ionic strength.

The negligible influence of the ionic strength and headgroup contradicts the prediction based on the Gouy-Chapman theory given in Eq. (1). This deviation becomes less pronounced upon replacing the theoretically predicted surface potentials (see Introduction) with the considerably smaller experimental ones. In literature, pure PS vesicles are reported to have typical surface potentials of about 60 mV in the presence of 100 mM KCl, and of about 120 mV in the presence of 10 mM KCl [31,32]. However, these values yield still an additional repulsive tension of about 5.6 mN/m for 100 mM KCl, or 5.2 mN/m for 10 mM KCl. According to the finding of Ref. [15], this additional surface tension should still cause the rupture of most membranes, or should at least decrease their breakdown voltage significantly. Therefore from our experimental data it must be concluded that the stability of PS BLM is dominated by others than electrostatic forces.

TABLE III. Average breakdown voltages of POPC, POPS, DPhPC, and DPhPS membranes in aqueous media containing different KCl concentrations; $T = 295$ K. The number of experiments are indicated in the brackets. Errors given are standard errors.

	Average breakdown voltage 2 M KCl	Average breakdown voltage 100 mM KCl	Average breakdown voltage 10 mM KCl
POPC	455±7 mV (10)	400±6 mV (15)	420±23 mV (10)
POPS	480±20 mV (12)	410±20 mV (16)	435±25 mV (12)
DPhPC	527±12 mV (15)	546±15 mV (20)	565±25 mV (15)
DPhPS	525±25 mV (15)	530±15 mV (40)	530±25 mV (20)

TABLE IV. Average rupture velocities of POPC, POPS, DPhPC, and DPhPS membranes in aqueous media containing different KCl concentrations; $T = 295$ K. The number of experiments are indicated in the brackets. Errors given are standard errors.

Lipid	Average rupture velocity 2 M KCl	Average rupture velocity 100 mM KCl	Average rupture velocity 10 mM KCl
POPC	8±1 cm/s (10)	5±1 cm/s (15)	5±0.5 cm/s (10)
POPS	14±1 cm/s (12)	5±1 cm/s (16)	5±2 cm/s (12)
DPhPC	33±2 cm/s (15)	19±2 cm/s (20)	20±4 cm/s (15)
DPhPS	43±3 cm/s (15)	20±1.5 cm/s (40)	20±2 cm/s (20)

Influence of ionic strength on the rupture velocity

The rupture kinetics of the membranes was analyzed according to Eqs. (4)–(6). To evaluate the rupture velocities α, we used the following bulk conductivity: 0.14 S/m for 10 mM KCl, 1.4 S/m for 100 mM KCl, 11.2 S/m for 1 M KCl, 19.6 S/m for 2 M KCl, and 28 S/m for 3 M KCl [19] DPhPS or DPhPC membranes display very similar rupture velocities (Table IV). In 10 and 100 mM KCl, velocities of about 20 cm/s are detected. Therefore, the influence of the negative surface charge of DPhPS membranes on the pore conductivity during rupture is negligible. The pore widening kinetics of POPS and POPC membranes is also very similar. However, there are two striking observations. First, DPh membranes are disrupted with fourfold higher apparent velocities than PO membranes. This is surprising as PO and DPh bilayers should have a similar thickness and density and hence similar inertia. On basis of our model, one should therefore expect equal rupture velocities for the investigated membranes on the condition that the parameter Φ which depends on the unknown material flow and dissipation effects is the same for PO and DPh membranes.

In our model we assume the formation of a defect of circular shape. If more than one defect or noncircular shaped defect occur, our velocity represents an apparent rupture velocity. Within our model approach the shape of the defects is therefore inseparable from the rupture velocity. Recent investigation on soap films revealed star-shaped defects in the fast disrupting soap films [33,34]. Therefore the formation of noncircular defects in fast disrupting BLM seems possible. Moreover, taking the similar membrane capacitance of our DPh and PO membranes into account, it also seems very reasonable that these two membranes do not only have different mechanical properties, as indicated by their break-

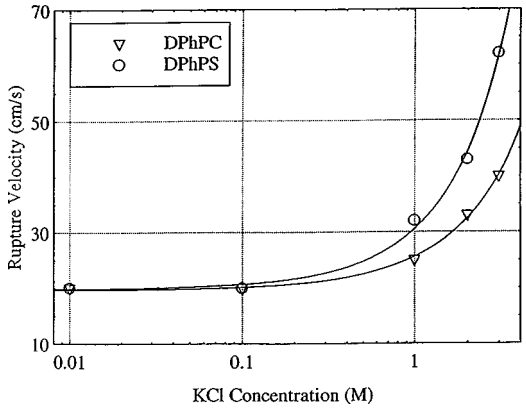

FIG. 3. Average rupture velocities of DPhPS and DPhPC membranes. The aqueous phase contained KCl concentrations between 10 mM and 3 M; $T = 295$ K. Note that the KCl concentration is plotted on a logarithmic scale.

down voltages, but may also form differently shaped defects while they disrupt. As the widening of a star-shaped defect dissipates more energy than the widening of a circular-shaped one [35], the finding of different rupture velocities in membranes of different mechanical stability seems plausible. With respect to our experiments, these considerations suggest that PO membranes form, upon electroporation, defects which do have more serrated edges than DPh membranes.

A second striking observation is the increase in the rupture velocity at higher ionic strength, which was observed for all lipids investigated in this study. In Fig. 3, we show the increasing rupture velocity for DPh membranes as a function of the bulk KCl concentrations. This increase cannot be attributed to a more frequent formation of multiple pores in media of high ionic strength, since the histograms of the rupture velocities show a narrow distribution of the rupture velocities for all ionic strengths investigated (compare Fig. 4). As the ionic strength increases, the velocities are shifted to higher values. One might think that the ionic strength-dependent time window of our method causes the changes in rupture velocities. We can detect the pore opening only up to the point where the *trans*-membrane voltage decays to zero. At low ionic strength the membrane discharges slowly, and the pore widening can be followed during a longer period in comparison to high ionic strength. The time window to record the kinetic of the breakdown in 10 mM KCl containing water is about several 100 μs, whereas it is reduced to $\sim$10 μs in 3 M KCl containing water. Close inspection of the conductivity curves, however, revealed constant slopes for all time intervals. In other words no decrease of the rupture velocities could be observed at longer times.

Another explanation could be that high KCl concentrations perturbate the water structure around the lipid headgroups. To check this possibility, we performed control experiments with other substances acting on the water activity, e.g., poly(ethylene-glycol) 2000 and 8 M urea. In contrast to high KCl concentrations, these two substances decreased the rupture velocities. Nevertheless the presence of high KCl concentrations again caused increased rupture velocities.

However, in our opinion the most reasonable explanation is that surface conductivity is the dominant pathway of membrane discharge. This would lead to an apparent slower rupture at low ionic strength, as observed in our experiments.

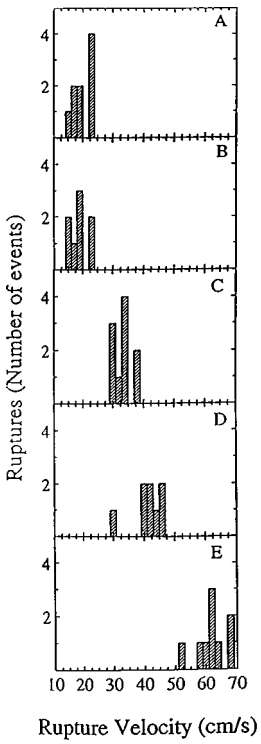

FIG. 4. Distribution of the rupture velocities of DPhPS membranes in bulk media of different ionic strength. Histogram *A* shows the frequency of the rupture events as a function of the rupture velocity for 10 mM KCl, histogram *B* for 100 mM KCl, histogram *C* for 1 M KCl, histogram *D* for 2 M KCl, and histogram *E* for 3 M KCl; $T = 295$ K.

CONCLUSIONS

We have shown that the breakdown voltages of BLM formed of negatively charged PS and zwitterionic PC lipids are not significantly different. Moreover, the breakdown voltages of PS membranes are the same in the presence of 100 and 10 mM KCl. These experimental observations suggest that the electrostatic repulsion of serine headgroups does not cause a significant additional stress in POPS and DPhPS membranes compared to POPC or DPhPC membranes. On the other hand, inserting experimental surface potentials of PS membranes into the Gouy-Chapman theory predicts so strong lateral stresses, that the membranes should disrupt. This prediction is in clear contrast to our observations.

The breakdown voltages of the membranes suggest stronger intermolecular links in DPh membranes compared to PO membranes. The analysis of the discharge process during membrane rupture suggests, on the basis of our model, apparently smaller pore widening velocities for PO than for DPh membranes. This discrepancy could be due to the formation of differently shaped defects in both membranes.

ACKNOWLEDGMENTS

We would like to thank Professor Gerhard Schwarz for his support. This work was sponsored by Grant Nos. 31.042045.94 and 7BUPJ048478 from the Swiss National Science Foundation.

[1] I. G. Abidor *et al.*, Bioelectrochem. Bioenerg. **6**, 37 (1979).
[2] R. Benz, F. Beckers, and U. Zimmermann, J. Membr. Biol. **48**, 181 (1979).
[3] M. Winterhalter, in *Nonmedical Application of Liposomes*, edited by D. D. Lasic and Y. Barenholz (CRC, Boca Raton, FL, 1997), p. 285.
[4] S. A. Freeman, M. A. Wang, and J. C. Weaver, Biophys. J. **67**, 42 (1994).
[5] *Electroporation and Electrofusion in Cell Biology*, edited by E. Neumann, A. E. Sowers, and C. A. Jordan (Plenum, New York, 1989).
[6] *Guide to Electroporation and Electrofusion*, edited by D. C. Chang *et al.* (Academic, New York, 1992).
[7] W. Sung and P. J. Park, Biophys. J. **73**, 1797 (1997).
[8] V. F. Antonov, E. Yu. Smirnova, and E. V. Shevchenko, Chem. Phys. Lipids **52**, 251 (1990).
[9] D. Needham and R. M. Hochmuth, Biophys. J. **55**, 1001 (1989).
[10] M. Winterhalter and W. Helfrich, J. Colloid Interface Sci. **122**, 583 (1988).
[11] V. F. Pastushenko and Yu. A. Chizmadhev, Gen. Physiol. Biophys. **1**, 43 (1982).
[12] R. W. Glaser *et al.*, Biochim. Biophys. Acta **940**, 275 (1988).
[13] A. Diederich, G. Bähr, and M. Winterhalter, Langmuir **14**, 4597 (1998).
[14] M. Winterhalter and W. Helfrich, J. Phys. Chem. **96**, 327 (1992).
[15] D. Needham and R. S. Nunn, Biophys. J. **58**, 997 (1990).
[16] H. Träuble, H. Erbl, and A. Blume, Biochim. Biophys. Acta **553**, 476 (1979).
[17] H. J. Galla and E. Sackmann, J. Am. Chem. Soc. **97**, 4114 (1975).
[18] A. Blume and H. Eibel, Biochim. Biophys. Acta **558**, 13 (1979).
[19] C. Wilhelm, M. Winterhalter, U. Zimmermann, and R. Benz, Biophys. J. **64**, 121 (1993).
[20] M. Lindemann, M. Steinmetz, and M. Winterhalter, Prog. Colloid Polym. Sci. **102**, 209 (1997).
[21] P. Mueller *et al.*, J. Phys. Chem. **67**, 534 (1963).
[22] C. Taupin, M. Dvolaitzky, and C. Sauterey, Biochemistry **14**, 4771 (1981).
[23] A. G. Petrov, *The Lyotropic State of Matter* (Gordon and Breach, New York, 1998).
[24] W. Harbich and W. Helfrich, Z. Naturforsch. A **24**, 1063 (1979).
[25] I. Genco *et al.*, Biochim. Biophys. Acta **1149**, 10 (1993).
[26] L. V. Chernomordik *et al.*, Biochim. Biophys. Acta **812**, 643 (1985).
[27] D. V. Zhelev and D. Needham, Biochim. Biophys. Acta **1147**, 89 (1993).
[28] M. Winterhalter and W. Helfrich, Phys. Rev. A **36**, 5874 (1987).
[29] B. Hille, *Ionic Channels of Excitable Membranes* (Sinauer, Sunderland, MA, 1984).
[30] K. H. Klotz, M. Winterhalter, and R. Benz, Biochim. Biophys. Acta **1147**, 161 (1993).
[31] Y. A. Ermakov, Biochim. Biophys. Acta **1023**, 91 (1990).
[32] M. Eisenberg, T. Gresafi, T. Riccio, and S. McLaughlin, Biochemistry **18**, 5213 (1979).
[33] L. J. Evers, S. Yu. Shulepov, and G. Frens, Faraday Discuss. **104**, 335 (1996).
[34] L. J. Evers, S. Yu. Shulepov, and G. Frens, Phys. Rev. Lett. **79**, 4850 (1997).
[35] J. C. Shillcock and D. H. Boal, Biophys. J. **71**, 317 (1996).